10

Wavelets in Medicine and Physiology

P. Ch. Ivanov[1], A. L. Goldberger[2], S. Havlin[1,3], C.-K. Peng[1,2],

M. G. Rosenblum[1], H. E. Stanley[1]

[1] *Center for Polymer Studies and Department of Physics, Boston University, Boston, MA 02215*

[2] *Cardiovascular Division, Harvard Medical School, Beth Israel Hospital, Boston, MA 02215*

[3] *Gonda-Goldschmied Center and Department of Physics, Bar-Ilan University, Ramat-Gan 52900, Israel*

Abstract: We present a combined wavelet and analytic signal approach to study biological and physiological nonstationary time series. The method enables one to reduce the effects of nonstationarity and to identify dynamical features on different time scales. Such an approach can test for the existence of universal scaling properties in the underlying complex dynamics. We applied the technique to human cardiac dynamics and find a universal scaling form for the heartbeat variability in healthy subjects. A breakdown of this scaling is associated with pathological conditions.

10.1 Introduction

The central task of statistical physics is to study macroscopic phenomena that result from microscopic interactions among many individual components. This problem is akin to many investigations undertaken in biology. In particular, physiological systems under neuroautonomic regulation, such as heart rate regulation, are good candidates for such an approach, since: (i) The systems often include multiple components, thus leading to very large numbers of degrees of freedom, and (ii) the systems usually are driven by competing forces. Therefore, it seems reasonable to consider the possibility that dynamical systems under neural regulation may exhibit temporal structures which are similar, under certain conditions, to those found in physical systems. Indeed, concepts and techniques originating in statistical physics are showing promise as useful tools for quantitative analysis of complicated physiological systems.

An unsolved problem in biology is the quantitative analysis of a nonstationary time series generated under free-running conditions [1–3]. The signals obtained under these constantly varying conditions raise serious challenges to both technical and theoretical aspects of time series analyses. A central

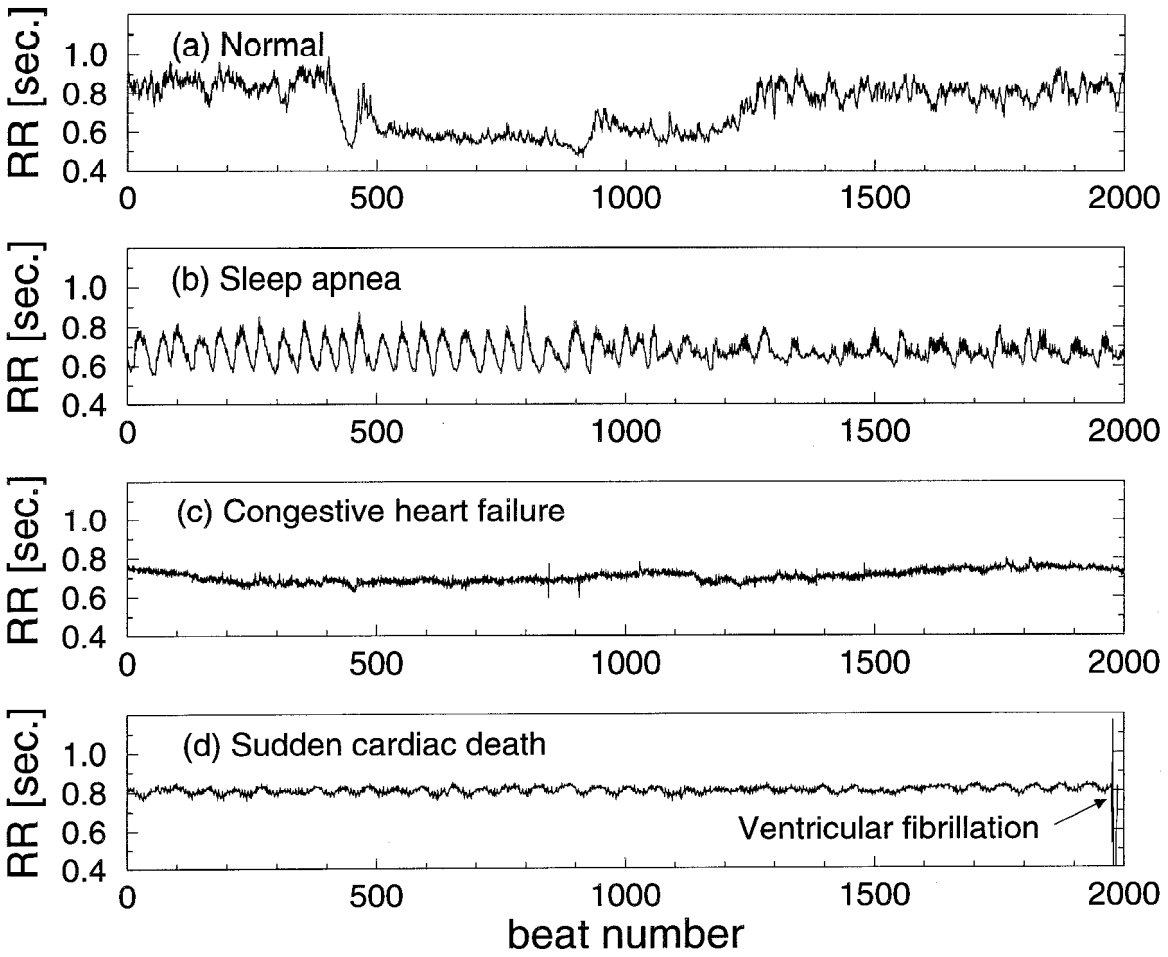

Fig. 10.1. Representative complex physiological fluctuations. Cardiac interbeat interval (normal sinus rhythm) time series of 2000 beats from (a) a healthy subject, (b) a subject with obstructive sleep apnea, (c) a subject with congestive heart failure and (d) a sudden cardiac death subject with ventricular fibrillation. Note the nonstationarity (patchiness) of these time series [most apparent in (a) and (b)]. Although these patches clearly differ in their amplitude and frequency of variations, their quantitative characterization remains an open problem and limits the applicability not only of traditional methods of analysis and modeling, but also newer techniques based on "chaos" theory.

question is whether such noisy fluctuating signals contain dynamical patterns essential for understanding underlying physiological mechanisms.

Representative examples of complex dynamical behavior under physiologic and pathologic conditions are shown in Fig. 10.1. Figure 10.1a shows a physi-

ologic cardiac interbeat time series—the output of a spatially and temporally integrated neuroautonomic control system. The time series shows erratic fluctuations and "patchiness". These fluctuations are usually ignored in conventional studies which focus on averaged quantities. In fact, these fluctuations are still often labeled as "noise" to distinguish them from the true "signal" of interest. Furthermore, these patterns change with pathological perturbations (shown in Figs. 10.1b–10.1d). However, with the recent adaption and extension of methods developed in statistical physics and nonlinear mathematics, it has been found that the physiological fluctuations shown in Fig. 10.1a exhibit an unexpected hidden scaling structure [4–7]. These findings raise the possibility that understanding the origin of such temporal structures and their alterations may (i) elucidate certain basic features of heart rate control mechanisms, and (ii) have practical value in clinical monitoring.

When analyzing complex cardiac fluctuations of the type shown in Fig. 10.1a, we must carefully exclude two obvious explanations for these observed structures: (i) they are simply an epiphenomenon of random (uncorrelated) trends, or (ii) they are a trivial consequence of the fact that cardiac function under neuroautonomic control is actually modulated by independent mechanisms with many time scales. To address the first possibility, researchers have recently developed and implemented methods to deal with the technical issue of nonstationarity in cardiac time series. To test the second possibility, numerically simulated systems with multiple time scales were studied, leading to the conclusion that robust scaling structures *cannot* be generated trivially from systems modulated by multiple time scales [8]. Instead, certain unique conditions are required to give the structures observed. Furthermore, these two "mechanisms" will not account for the observation of consistent changes in scaling patterns under pathological conditions, where complex nonstationarity and multiple time scale modulation are also present, but in altered form.

Among the difficulties associated with research on biomedical systems is not only the extreme variability of the signals but also the necessity of operating on a case-by-case basis. Often one does not know *a priori* which information is pertinent and on what scale it is located. Another important aspect of biomedical signals is that the information of interest is often a combination of features that are well-localized (temporally or spatially) and others that are more diffuse. As a result, the problems require the use of methods sufficiently robust to handle events that can be at opposite extremes in terms of their time-frequency localization. In the past few years, researchers have developed powerful wavelet methods for multiscale representation and analysis of signals [9–17]. These new tools differ from the

traditional Fourier techniques in that they localize information in the time-frequency plane and are especially suitable for the analysis of nonstationary data signals.

Due to the wide variety of signals and problems encountered in medicine and biology, the spectrum of applications of the wavelet transform has been extremely large. It ranges from signal processing analysis of physiological signals in bioacoustics (e.g., turbulent heart sounds) [18–27], electrocardiography [28–42], and electroencephalography [43–53] to applications for compression [54–57] and enhancement [58–60] in biomedical imaging, noise reduction [61–63], detecting microcalcifications in mammograms [64–69], detection and reconstruction techniques for X-ray tomography [70, 71], magnetic resonance imaging [72–75], positron emission tomography [76], human vision [77–80], and human DNA [81, 82]. Extensive reviews of these applications have been recently published [83–86].

In this chapter, we present a method to analyze the properties of human cardiac activity by means of a wavelet transform and analytic signal approach designed to address nonstationary behavior [7]. We find a universal scaling function for the distribution of the variations in the beat-to-beat intervals for healthy subjects. However, such a scaling function does not exist for a group with a cardiopulmonary instability due to sleep apnea (a condition in which breathing abnormalities during sleep affect cardiac activity). This scaling form allows us to express the global characteristics of a highly heterogeneous time series of interbeat intervals of each healthy individual with a single parameter. We find also that the observed scaling represents the Fourier phase correlations attributable to the underlying nonlinear dynamics. This approach has the potential to quantify the output of other nonlinear biological signals.

10.2 Nonstationary Physiological Signals

A time series is *stationary* if its statistical characteristics such as the mean and the variance are invariant under time shifts, i.e., if they remain the same when t is replaced by $t + \Delta$, where Δ is arbitrary. Then the probability densities, together with the moment and correlation functions, do not depend on the absolute position of the points on the time axis, but only on their relative configuration [87]. Non-stationarity, an important feature of biological variability, can be associated with regimes of different drifts in the mean value of a given signal, or with changes in its variance which may be gradual or abrupt.

Time series of beat-to-beat (RR) heart rate intervals [Fig. 10.2(a)] ob-

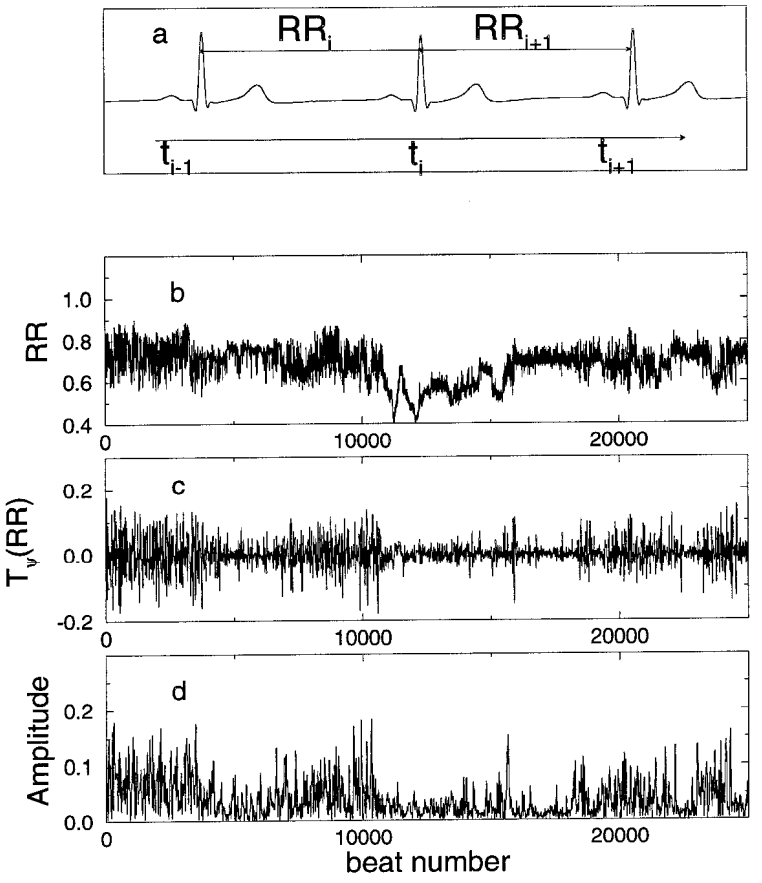

Fig. 10.2. (a) Segment of electrocardiogram showing beat-to-beat (RR_i) intervals. (b) Plot of RR-time series vs. consecutive beat number for a period of 6h ($\approx 2.5 \times 10^4$ beats). Nonstationarity (patchiness) is evident over both long and short time scales. (c) Wavelet transform $T_\psi(RR)$ of the RR-signal in (b) using the second derivative of the Gaussian function $\psi^{(2)}$ as analyzing wavelet with scale $a = 8$ beats. Nonstationarities related to constants and linear trends have been filtered. (d) Instantaneous amplitudes $A(t)$ of the wavelet-transform signal in (c); $A(t)$ calculated using the Hilbert transform measures the cumulative variations in the interbeat intervals over an interval proportional to the wavelet scale a.

tained from digitized electrocardiograms are known to be non-stationary and exhibit extremely complex behavior [88]. A typical feature of such nonstationary signals is the presence of "patchy" patterns which change over time [Fig. 10.2(b)]. The mechanism underlying this complex heart rate variability is related to competing neuroautonomic inputs [89, 90]. Parasympathetic stimulation decreases the firing rate of pacemaker cells in the heart's sinus node. Sympathetic stimulation has the opposite effect. The nonlinear interaction (coupling) of the two branches of the nervous system is the postulated mechanism for the type of erratic heart rate variability recorded in healthy subjects [91–93]. We focus our studies on interbeat interval variability as an important tool for elucidating possibly non-homeostatic cardiac variability because (i) the heart rate is under direct neuroautonomic control, (ii) interbeat interval variability is readily measured by non-invasive means, and (iii) analysis of these heart rate dynamics may provide important diagnostic and prognostic information.

Even under healthy, basal conditions, the cardiovascular system shows erratic fluctuations resembling those found in dynamical systems driven away from a single equilibrium state [94]. Do such "nonequilibrium" fluctuations [95] simply reflect the fact that physiological systems are being constantly perturbed by external and intrinsic noise? Or, do these fluctuations actually contain useful information about the underlying nonequilibrium control mechanisms?

Traditional approaches—such as the power spectrum and correlation analysis[96, 97]—are not suited for such nonstationary (patchy) sequences. In particular, they do not carry information stored in the Fourier phases which is crucial for determining nonlinear characteristics [98–100].

To address these problems, we develop a method—"cumulative variation amplitude analysis" (CVAA)—to study the subtle structure of physiological time series. This method comprises sequential application of a set of algorithms based on wavelet and Hilbert transform analysis.

10.3 Wavelet Transform

We first apply the wavelet transform [Fig. 10.2(c)], because it does not require stationarity and it preserves important Fourier phase information. The wavelet transform [9, 101, 102] of a time series $s(t)$ is defined as

$$T_\psi(t_0, a) \equiv \frac{1}{a}\int_{-\infty}^{+\infty} s(t)\psi\left(\frac{t-t_0}{a}\right)dt, \tag{10.1}$$

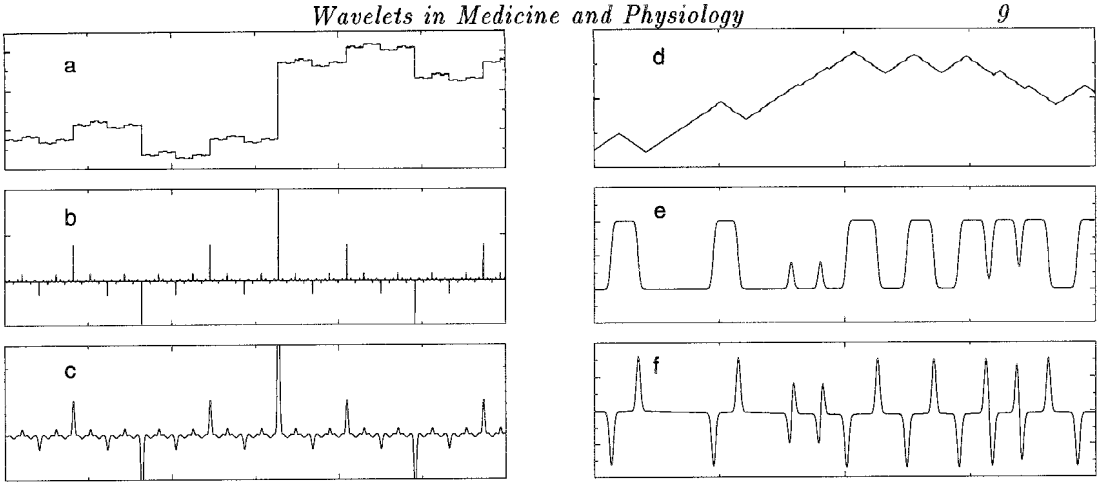

Fig. 10.3. Derivatives of the Gaussian function as analyzing wavelet extract the singularities (variations) from a signal with (a) constant and (d) linear trends. Wavelet transform of the signal in (a) using $\psi^{(1)}$ as analyzing wavelet with (b) smaller and (c) larger time scale. (e) $\psi^{(1)}$ and (f) $\psi^{(2)}$ are used on the signal in (d) at the same time scale.

where the analyzing wavelet ψ has a width of the order of the scale a and is centered at t_0. The wavelet transform is sometimes called a "mathematical microscope" because it allows one to study properties of the signal on any chosen scale a. For high frequencies (small a), the ψ functions have good localization (being effectively non-zero only on small sub-intervals), so short-time regimes or high-frequency components can be detected by the wavelet analysis. However, a wavelet with too large a value of scale a (low frequency) will filter out almost the entire frequency content of the time series, thus losing information about the intrinsic dynamics of the system. We focus our "microscope" on a scale $a = 8$ beats which smooths locally very high-frequency variations and best probes patterns of duration 30 sec to 1 min. The wavelet transform is attractive because it can eliminate local polynomial behavior (trends) in the nonstationary signal by an appropriate choice of the analyzing wavelet ψ [103].

In our study we use derivatives of the Gaussian function,

$$\psi^{(n)} \equiv \frac{d^n}{dt^n} e^{-\frac{1}{2}t^2}. \tag{10.2}$$

The first derivative is orthogonal to segments of the time series with an approximately constant local average. This results in fluctuations of the wavelet transform values around zero with highest spikes at the positions

where a sharp transition occurs [Fig. 10.3(b)]. Thus, the larger spikes indicate the boundaries *between* regimes with different local average in the signal, and the smaller fluctuations represent variations of the signal within a given regime. With increasing wavelet scale a, the fluctuations become broader and reflect the dominant structures (variations) in the signal [Fig. 10.3(c)] Since $\psi^{(1)}$ is not orthogonal to linear (non-constant) trends, the presence of consecutive linear trends [Fig. 10.3(d)] in the RR-intervals will give rise to fluctuations of the wavelet transform values around different nonzero levels corresponding to the slopes of the linear trends [Fig. 10.3(e)]. The second derivative $\psi^{(2)}$ of the Gaussian function and higher order derivatives can eliminate the influence of linear as well as nonlinear trends in the fluctuations of the wavelet transform values [Fig. 10.3(f)].

The wavelet transform allows one to "extract" from the data particular features. The object is to probe the *variations* in the heart rate signal at different time scales. The particular choice of the derivatives of the Gaussian function as analyzing wavelets allows us to extract these variations. One can argue that the same can be done by simply subtracting consecutive interbeat intervals by analyzing the increments only, but such standard analysis does *not* distinguish healthy from unhealthy cardiac dynamics [5]. The reason is that the wavelet transform in addition to extracting the variations over given time-scale in the heart rate signal reduces masking effects of the non-stationarities since the analyzing wavelet is orthogonal to local polynomial trends. The wavelet also filters out the very high-frequency noise in the original signal, preserving at the same time the sharpness of the edges separating different patterns in the signal, thus minimizing possibly artificial errors in the statistical analysis. Moreover, we find that the scale of the wavelet is crucial for extracting the *hidden* patterns in the cardiac dynamics. Thus, the ability of the wavelet transform to probe the signal on different scales is important for detecting essential features of cardiac dynamics under healthy as well as pathologic conditions.

The wavelet transform is thus a cumulative measure of the variations in the heart rate signal over a region proportional to the wavelet scale a, so the study of the behavior of the wavelet values can reveal intrinsic properties of the dynamics masked by nonstationarity.

10.4 Hilbert Transform

The wavelet transform signal at a fixed scale [Fig. 10.2(c)] shows segments of different duration and amplitudes. So the next step of the CVAA is to extract the amplitudes of the variations in the beat-to-beat signal by means

of an analytic signal approach [96, 104] which also does *not* require stationarity. This general approach, based on the Hilbert transform and originally introduced by Gabor [105], unambiguously gives the instantaneous phase and amplitude for a given signal $s(t)$ (in our case the wavelet transform of the interbeat interval time series) via construction of the analytic signal $S(t)$, which is a complex function of time defined as

$$S(t) \equiv s(t) + i\tilde{s}(t) = A(t)e^{i\phi(t)}. \tag{10.3}$$

Here $\tilde{s}(t)$ is the Hilbert transform of $s(t)$,

$$\tilde{s}(t) = \pi^{-1}\mathrm{P.V.}\int_{-\infty}^{+\infty} \frac{s(\tau)}{t-\tau}d\tau \tag{10.4}$$

where P.V. means that the integral is taken in the sense of the Cauchy principal value. The amplitude is defined as

$$A(t) \equiv \sqrt{s^2(t) + \tilde{s}^2(t)} \tag{10.5}$$

and the phase as

$$\phi(t) \equiv \tan^{-1}\left(\tilde{s}(t)/s(t)\right). \tag{10.6}$$

The Hilbert transform $\tilde{s}(t)$ of $s(t)$ can be considered as the convolution of the functions $s(t)$ and $1/\pi t$. This means that the Hilbert transform can be realized by an ideal filter whose amplitude response is unity, and phase response is a constant $\pi/2$ lag at all frequencies ([96]). A harmonic oscillation $s(t) = A\cos\omega t$ is often represented in the complex notation as $A\cos\omega t + jA\sin\omega t$. This means that the real oscillation is complemented by the imaginary part which is delayed in phase by $\pi/2$, and which is related to $s(t)$ by the Hilbert transform. The analytic signal is the direct and natural extension of this technique, as the Hilbert transform performs the $-\pi/2$ phase shift for every frequency component of an arbitrary signal.

Why do we need the instantaneous amplitude (envelope) of the signal? Suppose that our wavelet transform signal for a given scale consists of two segments (patches), both being sine waves with the amplitudes A and A'. Then the values of the signal for the first patch are distributed from $-A$ to A, and for the second patch from $-A'$ to A' $(A' > A)$. So the distributions of the data points values along the two patches of the signal overlap between $-A$ and A. However, if we consider the distributions of the instantaneous amplitudes of the data points from these two segments, then they *do not* overlap; they are, actually, two points, $P(A)$ and $P(A')$ with values reflecting the number of data points in each segment [Fig. 10.4]. By changing the wavelet scale we can learn about the distribution of patches with different duration.

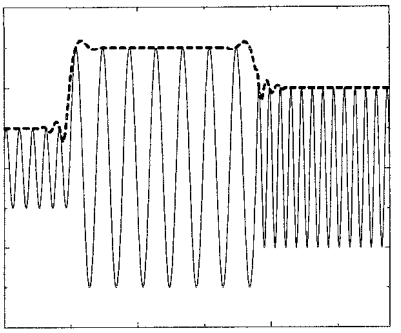

Fig. 10.4. Segments of sinusoidal signal with different frequencies and amplitudes (solid line) and their envelope obtained from Hilbert transform (dashed line).

10.5 Universal Distribution of Variations

Quantifying the probability distribution of variation amplitudes in the interbeat intervals can provide insights into the underlying dynamical processes because the distribution of interbeat intervals is directly related to the mechanisms which control heart rate variability. Therefore, by finding consistent features of the distribution which are robust with respect to different healthy subjects, we can quantify physiologic dynamics. However there are important technical difficulties which must first be overcome before such robust features can be found.

Among the possible reasons why an interbeat interval histogram can differ from case to case are: (i) Histograms can differ because they have different means and standard deviations but follow the same functional form. (ii) Histograms are described by different functional forms i.e., they belong to different classes of processes. The first type of difference is commonly observed (especially in physiological data where significant variation between individuals is expected) and should be taken care of by properly "renormalizing" (with respect to the mean and standard deviation) the histogram. If we assume that heart rate control mechanisms in healthy subjects follow the same general set of dynamical rules, then we expect that some variables of the system's output will be described by a single, well-defined distribution function. Functional differences between distributions, on the other hand, can be a result of altered mechanisms, and could be indicative of pathological behavior.

We analyzed the distribution of the amplitudes of the beat-to-beat varia-

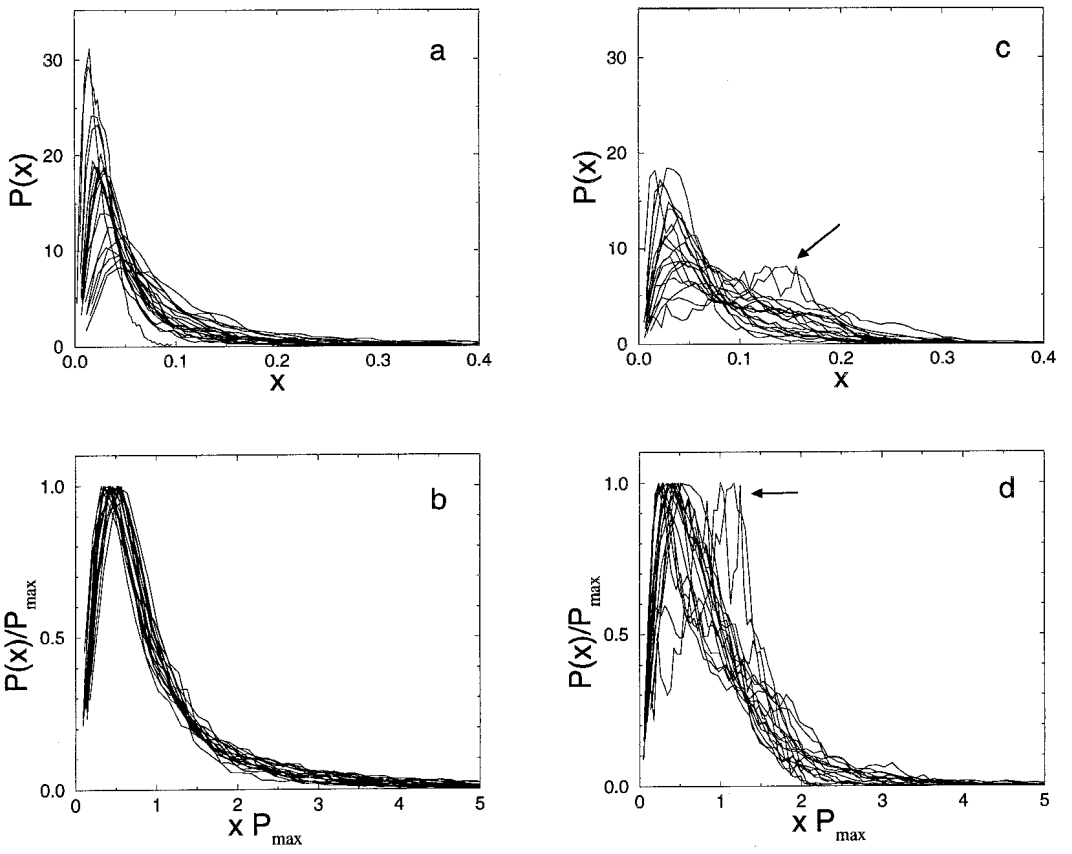

Fig. 10.5. (a) Probability distributions $P(x)$ of the amplitudes of heart rate variations $x \equiv A(t)$ for a group of 18 healthy adults (after wavelet transform with $\psi^{(2)}$ and scale $a = 8$ beats). Individual differences are reflected in the different average value and widths (standard deviations) of these distributions. All distributions are normalized to unit area. (b) Same probability distributions as in (a) after rescaling: $P(x)$ by $P_{\max}$, and x by $1/P_{\max}$ to preserve the normalization to unit area. This rescaling is equivalent to the scaling procedure discussed in the text (Eq. 10.9), since $P(x) \equiv P(x, b)$ and $P_{\max} \propto b$. We are able to describe the distributions using a single curve, indicating a robust, consistent scaling mechanism for the nonequilibrium dynamics. (c) Probability distributions for a group of 16 subjects with obstructive sleep apnea. We note that the second (rightward) peak (arrow) in the distributions for the sleep apnea subjects corresponds to the transient emergence of characteristic pathologic oscillations in the heart rate associated with periodic breathing (Fig. 10.1b). (d) Distributions for the apnea group after the same rescaling as in (b). These distributions *cannot* be well described by a single curve, indicating that the nonequilibrium dynamics are altered.

tions [Fig. 10.2(d)] for a group of healthy subjects ($N = 18$: 5 males and 13 females; age 20–50, mean 34) and a group of subjects [106] with obstructive sleep apnea [107, 108] ($N = 16$ males; age 32–56, mean 43). To minimize nonstationarity due to changes in the level of activity, we begin by considering night phase (12 P.M.–6 A.M.) records of interbeat intervals ($\approx 10^4$ beats) for both groups.

Inspection of the distribution functions of the amplitudes of the cumulative variations reveals marked differences between individuals [Fig. 10.5(a)]. These differences are not surprising given the underlying physiological differences among healthy subjects.

For the healthy group, we find that these distributions are well fit by the *generalized homogeneous* form [109] (the Gamma distribution):

$$P(x, b) = \frac{b^{\nu+1}}{\Gamma(\nu + 1)}\, x^{\nu} e^{-bx}, \tag{10.7}$$

where $b \equiv \nu/x_0$, $\Gamma(\nu+1)$ is the Gamma function, x_0 is the position of the peak $P = P_{\max}$, and ν is a fitting parameter [Fig. 10.6(a)]. A function $P(x, b)$ is a generalized homogeneous function if there exist two numbers α and β—called scaling powers—such that for all positive values of the parameter λ

$$P(\lambda^{\alpha} x, \lambda^{\beta} b) = \lambda P(x, b). \tag{10.8}$$

Generalized homogeneous functions are defined as solutions of this functional equation. One can see that in our case, $P(x, b)$ satisfies (10.8) with $\alpha = -1$ and $\beta = 1$.

Functions describing physical systems near their critical points are known to be generalized homogeneous functions [110]. Data collapse is among the key properties of generalized homogeneous functions. Instead of data points falling on a family of curves, one for each value of b, data points can be made to *collapse* onto a single curve given by the scaling function

$$\tilde{P}(u) \equiv \frac{P(x, b)}{b}, \tag{10.9}$$

where the number of independent variables is reduced by defining the scaled variable $u \equiv bx$. Our results show that a *common scaling* function $\tilde{P}(u)$ defines the probability density of the magnitudes of the variations in the beat-to-beat intervals for each healthy subject. Note that it is sufficient to specify *only one* parameter b in order to characterize the heterogeneous heartbeat variations for *each subject* in this group.

To test the hypothesis that there is a hidden, possibly universal, structure to these heterogeneous time series, we rescale the distributions and find

for all healthy subjects that the data conform to a single scaled plot ("data collapse") [Fig. 10.5(b)]. Such behavior is reminiscent of a wide class of well-studied physical systems with universal scaling properties [110, 111]. In contrast, the subjects with *sleep apnea* show individual probability distributions that *fail* to collapse [Fig. 10.5(d)]. The collapse of the individual distributions for all healthy subjects after rescaling their "individual" parameter is indicative of a "universal" structure. The term "universal" is used in the sense that a closed mathematical scaling form is established describing in a unified quantitative way the cardiac dynamics of all studied healthy subjects.

An analysis of the heart rate dynamics for healthy subjects during the daytime (noon–6 P.M.) indicates that the observed, apparently universal, behavior holds not only for the night phase but for the day phase as well [Fig. 10.6(b)]. Semilog plots of the averaged distributions show a systematic deviation from the exponential form (slower decay) in the tails of the night-phase distributions, whereas the day-phase distributions follow the exponential form over practically the entire range. Note that the tail of the observed distribution for the night phase indicates higher probability of larger variations in the healthy heart dynamics during sleep hours in comparison with the daytime dynamics.

We observe for the healthy group good data collapse with a *stable* scaling form for wavelet scales $a = 2$ up to $a = 64$ [Fig. 10.6(c)]. However, for very small scales ($a = 1, 2$) the group average of the rescaled distributions of the apnea subjects is indistinguishable from the average of the rescaled distributions of the healthy group. Thus, very high frequency variations are equally present in the signals from both groups. Our analysis yields the most robust results when a is tuned to probe the collective properties of patterns with duration of $\approx \frac{1}{2} - 1$ min in the time series ($a = 8, 10$). The subtle difference in the tail of the distributions between day and night phases is also best seen for this scale range.

We note that direct analysis of interbeat interval histograms does *not* lead to data collapse or separation between the healthy and apnea group. Such histograms measured directly for each subject do not converge to a single representative curve describing healthy dynamics, because the interbeat interval time series is highly nonstationary. Even rescaling the time series to give all histograms identical means and variances does not lead to a common curve for the histograms. Moreover, the direct application only of the Hilbert transform yielding the probability distribution of the instantaneous amplitudes of the original signal does *not* distinguish clearly healthy from abnormal cardiac dynamics. Hence, the wavelet transform, with its ability to

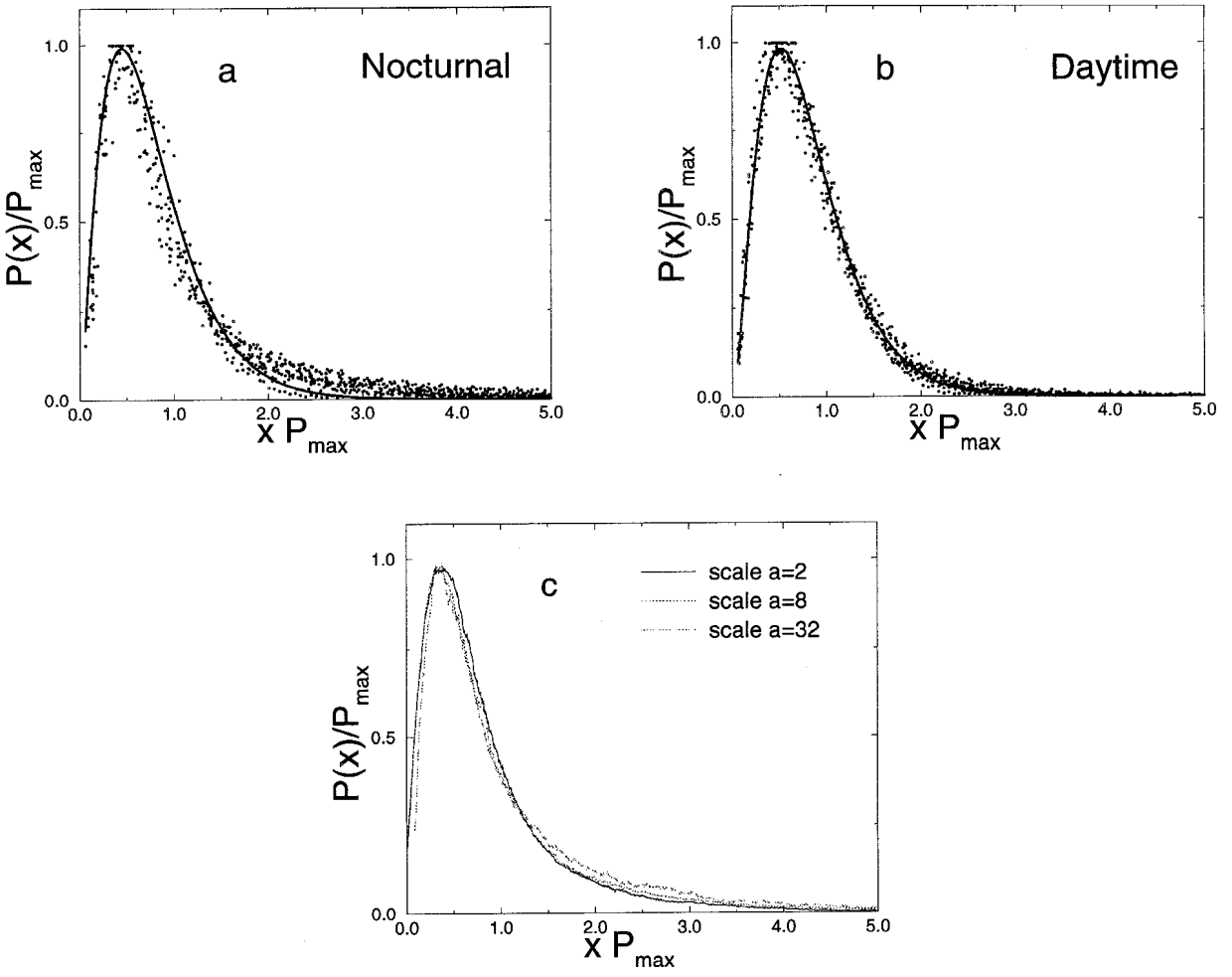

Fig. 10.6. (a) The solid line is an analytic fit of the rescaled distributions of the beat-to-beat variation amplitudes of the 18 healthy subjects during sleep hours to a stable Gamma distribution with $\nu = 1.4 \pm 0.1$. (b) Data for 6h records of RR intervals for the day phase of the same control group of 18 healthy subjects demonstrate similar scaling behavior with a Gamma distribution and $\nu = 1.8 \pm 0.1$, thereby showing that the observed common structure for the healthy heart dynamics is not confined to the nocturnal phase. (c) Group average of the rescaled distributions of the cumulative variation amplitudes for the healthy individuals during nocturnal hours. Note that the observed Gamma scaling is *stable* for a wide range of the wavelet transform scales a.

be orthogonal to polynomial trends and to probe the signal on different time scales, proves crucial to extract dynamical properties hidden in the cumulative variations, since different patterns can be observed on different time scales.

10.6 Wavelets and Scale Invariance

Differences between healthy and abnormal cardiac dynamics are known to be reflected in different correlations and power spectra [4–6, 97]. However, it is currently widely assumed in the literature that the difference in time series of interbeat intervals in sick and healthy adults *lies not in the distribution of the interbeat variations but rather in their time ordering.* This assumption is based on more conventional studies of interbeat increments [112]. These studies essentially amount to taking derivatives of the heart rate signal and thus extracting pointwise characteristics. Also, it has been hypothesized that even if the interbeat variations are different (e.g. smaller) during illness, the pattern of heart rate variability might be otherwise very similar to that during health, so that the interbeat variations for normal and abnormal cardiac dynamics, once normalized, would have the same distribution. Our study clearly rejects this hypothesis, showing the presence of scaling in the distributions of the variation amplitudes for the healthy [Fig. 10.5(b)] and a breakdown of this scaling for abnormal dynamics [Fig. 10.5(d)]. Moreover, the stability of this scaling form [Fig. 10.6(c)] indicates that the underlying dynamical mechanisms regulating the healthy heart beat have similar statistical properties on different time scales. Such statistical self-similarity is an important characteristic of fractal objects [98, 113]. The wavelet decomposition of beat-to-beat heart rate signals can be used to provide a visual representation of this fractal structure [Fig. 10.7]. The wavelet transform, with its ability to remove local trends and to extract interbeat variations on different time scales, enables us to identify self-similar patterns (arches) in these variations even when the signals change as a result of background interference. Data from sick heart lack these patterns. Fractal characteristics of the cardiac dynamics and other biological signals can be successfully studied with the generalized multifractal formalism based on the wavelet transform modulus maxima method (WTMM) presented in Chapter 9.

Similar time scale invariance was observed in the experiments of Rodieck on the interspike intervals of a single neuron cell which distribution was analyzed by Gerstein and Mandelbrot [114]. For several types of singe neuron cells Gerstein and Mandelbrot find that the interspike intervals distributions remain invariant with the time scale. However the heartbeat variations, un-

like the single neuron dynamics, represent the integrated output of spatially and temporally distributed feedback system.

Analysis of the variance of the distributions for healthy cardiac dynamics at different time scales shows a power law behavior with an exponent close to zero. This relates to previous studies reporting long-range anticorrelations in the heartbeat variations [5]. The findings that correlation functions and distributions describing physiological systems are not characterized by a single time scale become more plausible if we consider the survival advantage conferred upon organisms that evolved with an infinite hierarchy of time scales compared to organisms that evolved with a single characteristic time scale. Organisms with a physiologic control system generated by a single time scale are analogous, formally, to the famous Tacoma Narrows bridge, which survived many years until by chance a wind storm occurred that happened to correspond to the characteristic frequency (inverse of the characteristic time scale). Organisms that have survived millions of years have plausibly evolved some feature to render them immune from the analog of the Tacoma bridge disaster, and this feature would seem to be the absence of any characteristic time scales (compare Fig. 10.1(a) with 10.1(b) and 10.1(d), which show pathologic mode-locking).

10.7 A Diagnostic for Health vs. Disease

We employ the Kolmogorov-Smirnov test to measure how similar two probability distributions are. A mathematical relation exists which links the Kolmogorov-Smirnov parameter D(KS) to the corresponding statistical significance level [115]. The larger the value of $D(KS)$, the more unlikely the two data sets were obtained from the same probability distribution (the null hypothesis).

The Kolmogorov-Smirnov test provides a simple measure that is defined as the *maximum value* of the absolute difference between two cumulative distribution functions.

The K-S test is defined as follows:

(i) Once the probability distribution $P(x)$ is found for a subject which we want to compare to a fit $P_0(x)$, the cumulative probability distribution $W(x)$ for the subject is found using the relation

$$W(x) \equiv \int_0^x P(x')dx',$$

and similarly for the the cumulative probability distribution $W_0(x)$ of the fit $P_0(x)$.

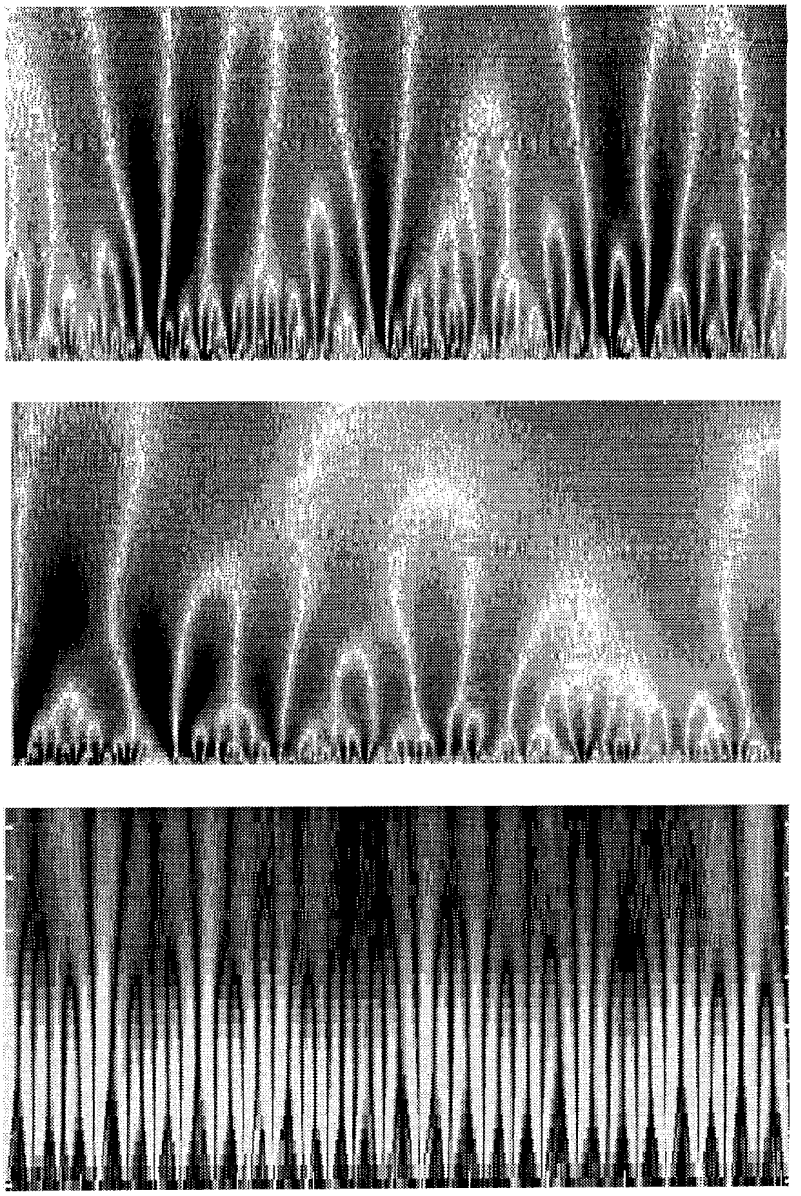

Fig. 10.7. Color coded wavelet analysis of RR signals. The x-axis represents time ($\approx$ 2000 beats) and the y-axis indicates the scale of the wavelet used ($a = 1, 2, \ldots, 60$) with large scales at the top. The brighter colors indicate larger values of the wavelet amplitudes. The wavelet analysis performed with $\psi^{(2)}$ (the Mexican hat) as an analyzing wavelet uncovers a hierarchical scale invariance (top panel) quantitatively expressed by the stability of the scaling form on Fig. 10.6(c). This wavelet decomposition reveals a self-similar fractal structure in the healthy cardiac dynamics — a magnification of the central portion of the top panel with 200 beats on the x-axis and wavelet scale $a = 1, 2, \ldots, 25$ on the y-axis shows identical branching patterns (middle panel). Loss of this fractal structure in cases with sleep apnea (lower panel).

(ii) The absolute difference $\Delta W(x) \equiv |W(x) - W_0(x)|$ is found.

(iii) The maximum value of this absolute difference is defined as the K-S parameter [Fig. 10.8(b)]: $D(KS) \equiv \max[\Delta W(x)]$.

Once the distributions for the subjects and a fit for healthy subjects are found, we apply the K-S test to see how different each subject's distribution is from the fit. Comparing the individual distributions of the healthy and sleep apnea subjects with the reported scaling form [Eq. (10.9)] for the healthy dynamics, we find that the Kolmogorov-Smirnov test can serve as a potentially useful tool to separate healthy from abnormal cardiac dynamics [Fig. 10.8(a)]. The question of diagnostics motivates us to look more closely at the first and second moments of the distributions of the variation amplitudes for both groups. We find that a simple presentation of the values for these moments can be also effectively used to separate quantitatively the two groups. We present these results in [Fig. 10.8(b)]—the first and second moments of the healthy distributions exhibit lower values with good linear fit, whereas for the apnea group these values are higher and dispersed with almost no overlap with the healthy data.

10.8 Information in the Fourier Phases

Correlation functions measure how the value of some function depends on its value at an earlier time. Many simple systems in nature have correlation functions that decay with time in an exponential way. For systems comprised of many interacting subsystems, physicists discovered that such exponential decays do not occur. Rather, correlation functions were found to decay with a power law form. The implication of this discovery is that in complex systems, there is no single characteristic time [119, 120]. If correlations decay with a power-law form, we say the system is "scale free" since there is no characteristic scale associated with a power law. Since at large time scales a power law is always larger than an exponential function, correlations described by power laws are termed "long-range" correlations—they are of longer range than exponentially-decaying correlations.

In physiological systems, recent work has suggested that such "long-range" power-law correlations occur in a range of physiological systems [118, 121, 122] including, most remarkably, the intervals between successive heartbeats [5, 6]. The discovery of long-range correlations in these intervals is all the more interesting because it appears that these correlations are not present in certain disease states.

What are the possible adaptive advantages of the apparently far-from-

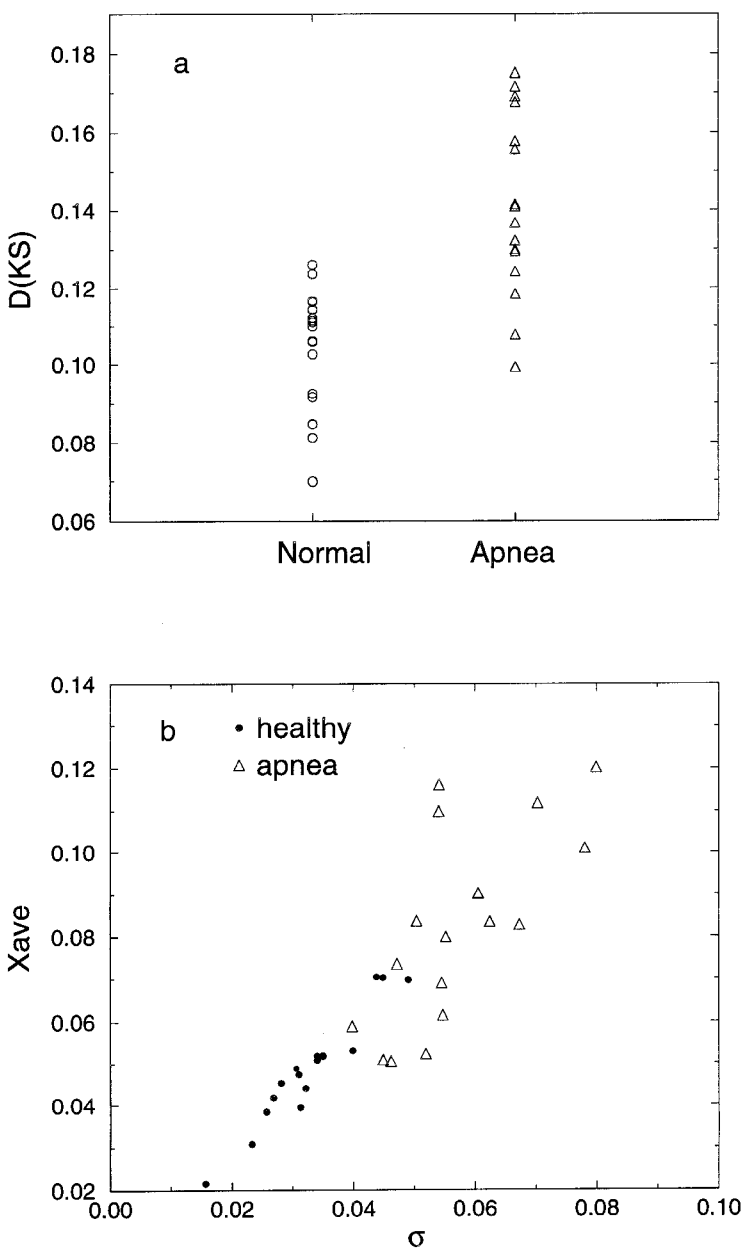

Fig. 10.8. (a)The Kolmogorov-Smirnov parameter $D(KS)$ and (b) the values of the first moments (mean and standard deviation σ) of the cumulative variation amplitude distributions can be used as a diagnostic of the healthy vs. apnea subjects with more then 80% true-positive recognition.

equilibrium behavior that appears to characterize the free-running dynamics of certain neural control systems? First, we note that complex erratic fluctuations shown in Fig. 10.1(a) are *not* inconsistent with the general concept that physiological systems must operate with certain bounds. However, an intriguing possibility is that these complex nonequilibrium dynamics, rather than classical homeostatic *constancy*, may be a mechanism for maintaining physiologic stability. Such complex multi-scale variability keeps the system from becoming locked to a dominant frequency (mode locking), a common manifestation of pathologic dynamics [Fig. 10.1(b)]. At the same time, long-range fractal correlations underlying these complex fluctuations may provide an important organizational mechanism for systems that lack a characteristic spatial or temporal scale. Finally, the intrinsic "noisiness" of far-from-equilibrium dynamics may facilitate coping with unpredictable environmental stimuli.

However, these fractal correlations detected by Fourier and fluctuation analysis techniques, ignore information related to the phase interactions of component modes. The nonlinear interaction of these modes accounts for the visually "patchy" appearance of the normal heartbeat time series.

To ascertain whether the observed scaling of the distributions for healthy subjects is an intrinsic property of normal heart beat dynamics, we test the cumulative variation amplitude analysis on artificially-generated signals with known properties. Our analysis of uniformly-distributed random numbers in the interval $[0, 1]$ and of Gaussian-distributed noise with and without long-range power law correlations shows that after the wavelet transform the amplitude distributions follow the Rayleigh probability distribution

$$R(x) = \left(\frac{x}{\sigma^2}\right) e^{-x^2/\sigma^2}.$$

This finding agrees with the central limit theorem, which can be expressed as a property of convolutions (in our case wavelet transforms): the convolution of a large number of positive functions is approximately a Gaussian function, and the instantaneous amplitudes of a Gaussian process follow the Rayleigh probability distribution [87].

We perform parallel analysis on surrogate data obtained from a healthy subject by Fourier transforming the original time series, preserving the amplitudes of the Fourier transform but *randomizing the phases*, and performing an inverse Fourier transform [Fig. 10.9(c)]. Thus, both the original and surrogate signals have *identical* power spectra. Application of the CVAA method on this surrogate signal results again in a Rayleigh distribution, whereas the original time series has a distribution with an exponential tail. This test

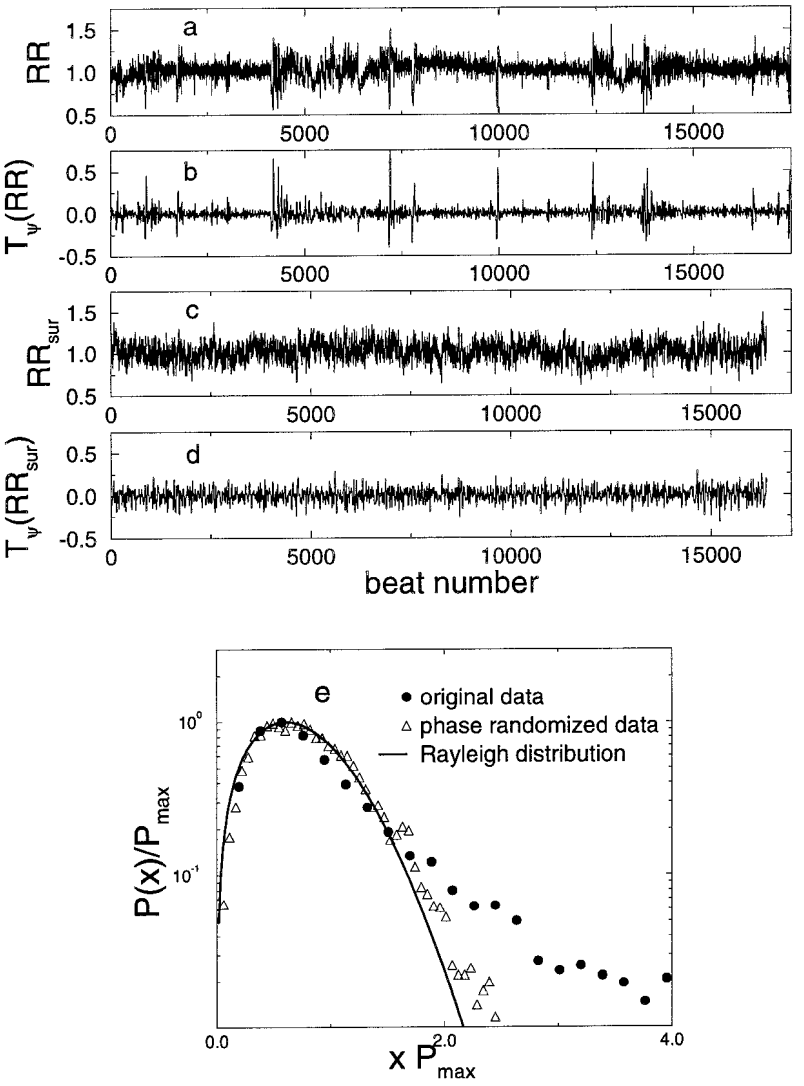

Fig. 10.9. (a) Original time series RR as a function of beat number. (b) Wavelet transform $T_\psi(RR)$ of this series. (c) Surrogate signal (RR_{sur}) after phase randomization. (d) Wavelet transform of the surrogate signal which is more homogeneous (less patchy) in comparison with (b). (e) Probability distributions of the amplitudes of variations after wavelet transform of the original and surrogate signals, as well as the theoretical Rayleigh distribution. The theoretical Rayleigh agrees with the distribution of the wavelet transform of the surrogate signal with randomized phases.

clearly indicates the important role of *phase correlations* in the RR time series. The presence of these correlations is most likely related to the underlying nonlinear dynamics [117, 123]. The observed breakdown of this scaling pattern in the sleep apnea cases—a common and important instability of cardiopulmonary regulation—is possibly related to pathological mode locking associated with periodic breathing dynamics [116].

These tests show that the observed scaling in the variations of interbeat intervals for healthy dynamics actually represents the Fourier phase correlations. This result is non-trivial since it adds to an ongoing discussion about whether nonlinear phase interactions are present in healthy cardiac dynamics [91]. Furthermore, this finding suggests that, for healthy individuals, there may be a common structure to this nonlinear phase interaction. Also, the tests demonstrate that the scaling is not an artificial result of our approach in that it gives the expected results for known processes, i.e., a Rayleigh distribution for the amplitudes of uniformly distributed random numbers and for Gaussian noise as well. The basis of this robust temporal structure remains unknown and presents a new challenge to the understanding of nonlinear mechanisms of heartbeat control.

10.9 Concluding Remarks

(i) Heart rate dynamics under normal conditions display nonequilibrium fluctuations that reveal a remarkable physiological structure when analyzed using wavelets and methods adapted from statistical physics.

(ii) There is a hitherto unknown scaling pattern to interbeat interval variations in healthy subjects. This finding allows us to express the global characteristics of the highly heterogeneous heart rate time series of each healthy individual with only a *single parameter*. This scaling property cannot be explained by activity, since we analyzed data from subjects during nocturnal hours. Moreover, it cannot be accounted for by sleep stage transitions, since we found a similar pattern during day-time hours.

(iii) This scaling is related to the intrinsic nonlinear dynamics of the control mechanism because it is due to information in the phase relationships. This information is *not* in the 1/f power spectrum on which all previous heart rate scaling is based, and any realistic attempt to model heart rate control will need to account for this scaling behavior.

(iv) The reported results are also the first that clearly show a *difference* in the distributions of the interbeat variations for normal and abnormal heart dynamics. However, to observe it, one must:

(a) properly reduce masking effects of nonstationarity;
(b) account for the importance of time scales to reveal *hidden* scaling.

In both aspects the wavelet analysis proves superior to other more conventional techniques.

(v) The observation of nonlinear dynamics is *not* accounted for by traditional physiological mechanisms and motivates new modeling strategies to understand nonequilibrium control systems under healthy and pathologic conditions.

(vi) The wavelet-based method we present can be applied to other complex, nonstationary time series.

ACKNOWLEDGEMENTS. We thank Alan Arneodo, Hernán A. Makse, Martin Meyer, Luis A. N. Amaral and Alison Hill for discussions. This work was supported by NIH, NIMH, NASA, Binational Science Foundation USA-Israel and The G. Harold and Leila Y. Mathers Charitable Foundation.

Bibliography

[1] G. E. P. Box, G. M. Jenkins and G. C. Reinsel, *Time series analysis: forecasting and control* (Prentice-Hall, Englewood Cliffs, 1994).

[2] M. F. Shlesinger, 'Fractal time and $1/f$ noise in complex systems,' *Ann. NY Acad. Sci.* **504**, 214–228 (1987).

[3] L. S. Liebovitch, 'Testing fractal and Maskov models of ion channel kinetics,' *Biophys. J.* **55**, 373–377 (1989).

[4] R. G. Turcott and M. C. Teich, 'Fractal character of the electrocardiogram: distinguishing heart-failure and normal patients,' *Ann. Biomed. Eng.* **24**, 269–293 (1996).

[5] C.-K. Peng, J. Mietus, J. M. Hausdorff, S. Havlin, H. E. Stanley and A. L. Goldberger, 'Long-range anti-correlations and non-Gaussian behavior of the heartbeat,' *Phys. Rev. Lett.* **70**, 1343–1346 (1993).

[6] C.-K. Peng, S. Havlin, H. E. Stanley and A. L. Goldberger, 'Quantification of scaling exponents and crossover phenomena in nonstationary heartbeat time series,' in *Proc. NATO dynamical disease conference*, edited by Glass L. *Chaos* **5**, 82–87 (1995).

[7] P. Ch. Ivanov, M. G. Rosenblum, C.-K. Peng, J. Mietus, S. Havlin, H. E. Stanley and A. L. Goldberger, 'Scaling behaviour of heartbeat intervals obtained by wavelet-based time-series analysis,' *Nature* **383**, 323–327 (1996).

[8] J. M. Hausdorff and C.-K. Peng, 'Multiscaled randomness: a possible source of $1/f$ noise in biology,' *Phys. Rev. E* **54**, 2154–2157 (1996).

[9] I. Daubechies, 'Orthonormal bases of compactly supported wavelets,' *Comm. Pure and Appl. Math.* **41**, 909–996 (1988).

[10] M. Vetterli and J. Kovacevic, *Wavelets and Subbane Coding* (Prentice-Hall, Englewood Cliffs NJ, 1995).

[11] H. Bray, K. McCormick, R. O. Wells, Jr. and X. D. Zhou, 'Wavelet variations on the Shannon sampling theorem,' *Biosystems* **34**, 249–257 (1995).

[12] H. L. Resnikoff, 'Analytic representation of compactly supported wavelets,' *Biosystems* **34**, 259–272 (1995).

[13] M. Fridman and J. M. Steele, 'Three statistical technologies with high potential in biological imaging and modeling,' *Basic Life Sci.* **63**, 199–224 (1994).

[14] G. Mayer-Kress, 'Localized measures for nonstationary time-series of physiological data,' *Integr. Physiol. Behav. Sci.* **29**, 205–210 (1994).

[15] L. Keselbrener ans S. Akselrod, 'Time-frequency analysis of transient signals — application to cardiovascular control' *Physica A* (1997) in print.

[16] T. A. Gyaw and S. R. Ray, 'The wavelet transform as a tool for recognition of biosignals,' *Biomed. Sci. Instrum.* **30**, 63–68 (1994).

[17] S. Mallat and W. L. Hwang,' 'Singularity detection and processing with wavelets,' *IEEE Trans. Inform. Theory* **38**, 617–643 (1992).

[18] M. Akay, Y. M. Akay, W. Welkowitz and S. Lewkowicz, 'Investigating the effects of vasodilator drugs on the turbulent sound caused by femoral artery stenosis using short-term Fourier and wavelet transform methods,' *IEEE Trans. Biomed. Eng.* **41**, 921–928 (1994).

[19] L. Khadra, M. Matalgah, B. el-Asir and S. Mawagdeh, 'The wavelet transform and its applications to phonocardiogram signal analysis,' *Med. Inf. (London)* **16**, 271–277 (1991).

[20] M. S. Obaidad, 'Phonocardiogram signal analysis: techniques and performance,' *J. Med. Eng. and Techol.* **17**, 221–227 (1993).

[21] C. Heneghan *et al.*, 'Investigating the nonlinear dynamics of cellular motion in the inner ear using the short-time Fourier and continuous wavelet transforms,' *IEEE Trans. Signal Process.* **42**, 3335–3352 (1994).

[22] W. J. Lammers, A. el-Kays, K. Arafat and T. Y. el-Sharkawy, 'Wave mapping: detection of co-existing multiple wavefronts in high-resolution electrical mapping,' *Med. Biol. Eng. Comput.* **33**, 476–481 (1995).

[23] E. G. Pasanen, J. D. Travis and R. J. Thornhill, 'Wavelet-type analysis of transient-evoked otoacoustic emissions,' *Biomed. Sci. Instrum.* **30**, 75–80 (1994).

[24] H. P. Wit, P. van Dijk and P. Avan, 'Wavelet analysis of real ear and synthesized click evoked otoacoustic emissions,' *Hear. Res.* **73**, 141–147 (1994).

[25] J. R. Bulgrin, B. J. Rubal, C. R. Thompson and J. M. Moody, 'Comparison of short-time Fourier, wavelet and time-domain analyses of intracardiac sounds,' *Biomed. Sci. Instrum.* **29**, 465–478 (1993).

[26] X. L. Xu, A. H. Tewfik and J. F. Greenleaf, 'Time delay estimation using wavelet transform for pulsed-wave ultrasound,' *Ann. Biomed. Eng.* **23**, 612–621 (1995).

[27] M. C. Teich, C. Heneghan, S. M. Khanna, A. Flock, M. Ulfendahl and L. Brundin, 'Investigating routes to chaos in the guinea-pig cochlea using the continuous wavelet transform and the short-time Fourier transform,' *Ann. Biomed. Eng.* **23**, 583–607 (1995).

[28] C. Li and C. Zheng, 'QRS Detection by wavelet transform,' in *Proc. Annu. Conf. on Eng. in Med. and Biol.* **15**, 330–331 (1993).

[29] L. Khadr, H. Dickhaus and A. Lipp, 'Representations of ECG late potentials in the time frequency plane,' *J. Med. Eng. & Technol.* **17**, 228–231 (1993).

[30] H. Dickhaus, L. Khadra and J. Brachmann, 'Time-frequency analysis of ventricular late potentials,' *Methods Inform. Med.* **33**, 187–195 (1994).

[31] O. Meste, H. Rix, P. Caminal and N. V. Thakor, 'Ventricular late potentials characterization in time-frequency domain by means of a wavelet transform,' *IEEE Trans. Biomed. Eng.* **41**, 625–634 (1994).

[32] L. Senhadji, G. Carrault, J. J. Bellanger and G. Passariello, 'Comparing wavelet transforms for recognizing cardiac patterns,' *IEEE Eng. in Med. and Biol. Mag.* **14**, 167–173 (1995).

[33] M. Karrakchou, C. V. Lambrecht and M. Kunt, 'Analyzing pulmonary capillary-pressure: more accurate using mutual wavelet packets for adaptive filtering,' *IEEE Eng. in Med. and Biol. Mag.* **14**, 179–185 (1995).

[34] Z. Li, B. J. Grant and B. B. Lieber, 'Time-varying pulmonary arterial input impedance via wavelet decomposition,' *J. Appl. Physiol.* **78**, 2309–2319 (1995).

[35] N. V. Thakor, X. R. Guo, Y. C. Sun and D. F. Hanley, 'Multiresolution wavelet analysis of evoked potentials,' *IEEE Trans. Biomed. Eng.* **40**, 1085–1094 (1993).

[36] D. Morlet, J. P. Couderc, P. Touboul and P. Rubel, 'Wavelet analysis of high-resolution ECGs in post-infarction patients: role of the basic wavelet and of the analyzed lead,' *Int. J. Biomed. Comput.* **39**, 311–325 (1995).

[37] A. B. Geva, H. Pratt and Y. Y. Zeevi, 'Spatio-temporal multiple source localization by wavelet-type decomposition of evoked potentials,' *Electroencephalogr. Clin. Neurophysiol.* **96**, 278–286 (1995).

[38] H. Dickhaus, L. Khadra and J. Brachmann, 'Quantification of ECG late potentials by wavelet transformation,' *Comput. Methods Programs Biomed.* **43**, 185–192 (1994).

[39] D. Morlet, F. Peyrin, P. Desseigne, P. Touboul and P. Rubel, 'Wavelet analysis of high-resolution signal-averaged ECGs in postinfarction patients,' *J. Electrocardiol.* **26**, 311–320 (1993).

[40] D. L. Jones, J. S. Touvannas, P. Lander and D. E. Albert, 'Advanced time-frequency methods for signal-averaged ECG analysis,' *J. Electrocardiol.* **25 Suppl.**, 188–194 (1992).

[41] L. Reinhardt, M. Mäkijärvi, T. Fetsch, J. Montonen, G. Sierra, A. Martínez-Rubio, T. Katila, M. Borggrefe and G. Breithardt, 'Predictive value of wavelet correlation functions of signal-averaged electrocardiogram in patients after anterior versus inferior myocardial infarction,' *J. Am. Coll. Cardiol.* **27**, 53–59 (1996).

[42] M. Karrakchou and M. Kunt, 'Multiscale analysis for singularity detection in pulmonary microvascular pressure transients,' *Ann. Biomed. Eng.* **23**, 562–573 (1995).

[43] M. Akay, Y. M. Akay, P. Cheng and H. H. Szeto, 'Investigating the effects of opioid drugs on electrocortical activity using wavelet transform,' *Biol. Cybern.* **72**, 431–437 (1995).

[44] M. Akay, Y. M. Akay, P. Cheng and H. H. Szeto, 'Time-frequency analysis of the electrocortical activity during maturation using wavelet transform,' *Biol. Cybern.* **71**, 169–176 (1994).

[45] S. J. Schiff, J. Milton, J. Heller and A. L. Weinstein, 'Wavelet transforms and surrogate data for electroencephalographic and seizure localization,' *Opt. Eng.* **33**, 2162–2169 (1994).

[46] S. J. Schiff, A. Aldroubi, M. Unser and S. Sato, 'Fast wavelet transformation of EEG,' *Electroencephalogr. Clin. Neurophysiol.* **91**, 442–455 (1994).

[47] I. Clark, R. Biscay, M. Echeverría and T. Virués, 'Multiresolution

decomposition of non-stationary EEG signals: a preliminary study,' *Comput. Biol. Med.* **25**, 373–382 (1995).

[48] V. J. Samar, K. P. Swartz and M. R. Raghuveer, 'Multiresolution analysis of event-related potentials by wavelet decomposition,' *Brain Cong.* **27**, 398–438 (1995).

[49] A. W. Przybyszewski, 'An analysis of the oscillatory patterns in the central nervous system with the wavelet method,' *J. Neurosci. Methods* **38**, 245–257 (1991).

[50] E. A. Bartnik and K. J. Blinowska, 'Wavelets: a new method of evoked potential analysis [letter],' *Med. Biol. Eng. Comput.* **30**, 125–126 (1992).

[51] R. Sartenc *et al.*, 'Using wavelet transform to analyze cardiorespiratory and electroencephalographic signals during sleep,' in *Proc. IEEE EMBS Workshop on Wavelets in Med. and Biol.* (Baltimore, 1994), pp. 18a–19a.

[52] M. Akay and H. H. Szeto, 'Investigating the relationship between fetus EEG, respiratory, and blood pressure signals during maturation using wavelet transform,' *Ann. Biomed. Eng.* **23**, 574–582 (1995).

[53] L. Senhadji, J. L. Dillenseger, F. Wendling, C. Rocha and A. Kinie, 'Wavelet analysis of EEG for three-dimensional mapping of epileptic events,' *Ann. Biomed. Eng.* **23**, 543–552 (1995).

[54] A. S. Lewis and G. Knowles, 'Image compression using the 2-D wavelet transform,' *IEEE Trans. Image Process* **1**, 244–250 (1992).

[55] M. Antonini, M. Barland, P. Mathieu and I Danbechies, 'Image coding using wavelet transform,' *IEEE Trans. Image Process* **1**, 205–220 (1992).

[56] J. A. Crowe, N. M. Gibson, M. S. Woolfson and M. G. Somekh, 'Wavelet transform as a potential tool for ECG analysis and compression,' *J. Biomed. Eng.* **14**, 268–272 (1992).

[57] J. G. Daugman, 'Complete discrete 2-D Gabor transforms in neural networks for image analysis and compression,' *IEEE Trans. Acoust., Speech and Signal Process.* **36**, 1169–1179 (1988).

[58] A. F. Laine and S. Song, 'Multiscale wavelet representations for mammographic feature analysis,' in *Proc. SPIE Conf. Mathemat. Methods in Med. Imag.* **1768**, 306–316 (1992).

[59] R. A. Kiltie, J. Fan and A. F. Laine, 'A wavelet-based metric for visual texture discrimination with applications in evolutionary ecology,' *Math. Biosci.* **126**, 21–39 (1995).

[60] D. M. Healy, J. Lu and J. B. Weaver, 'Two applications of wavelets and related techniques in medical imaging,' *Ann. Biomed. Eng.* **23**, 637–665 (1995).

[61] L. M. Lim, M. Akay and J. A. Daubenspeck, 'Identifying respiratory-related evoked-potentials,' *IEEE Eng. in Med. and Biol. Mag.* **13**, 174–178 (1995).

[62] O. Bertrand, J. Bohorquez and J. Pernier, 'Time-frequency digital filtering based on an invertible wavelet transform: an application to evoked potentials,' *IEEE Trans. Biomed. Eng.* **41**, 77–88 (1994).

[63] R. Carmona and L. Hudgins, 'Wavelet de-noising of EEG signals and identification of evoked response potentials,' in *Proc. SPIE Conf. Wavelet Applicat. in Signal and Image Process. II, Vol. 2303* (San Diego, July 1994), pp. 91–104.

[64] R. N. Strickland and H. I. Hahn, 'Detection of microcalcifications in mammograms using wavelets,' in *Proc. SPIE Conf. Wavelet Applicat. in Signal and Image Process. II, Vol. 2303* (San Diego, July 1994),

pp. 430–441.

[65] B. J. Lucier, M. Kallergi, W. Qian, R. A. De Vore, R. A. Clark, E. B. Saff and L. P. Clarke, 'Wavelet compression and segmentation of digital mammograms,' *J. Digit. Imaging* **7**, 27–38 (1994).

[66] W. Qian, M. Kallergi, L. P. Clarke, H. D. Li, P. Venugopal, D. Song and R. A. Clark, 'Tree structured wavelet transform segmentation of microcalcifications in digital mammography,' *Med. Phys.* **22**, 1247–1254 (1995).

[67] L. P. Clarke, M. Kallergi, W. Qian, H. D. Li, R. A. Clark and M. L. Silbiger, 'Tree-structured non-liner and wavelet transform for microcalcification segmentation in digital mammography,' *Cancer Lett.* **77**, 173–181 (1994).

[68] W. Qian *et al.*, 'Digital mammography: m-channel quadrature mirror filters (QMFs) for microcalcification extraction,' *Computerized Med. Imaging and Graphics* **18**, 301–314 (1994).

[69] D. Wei, H. P. Chan, M. A. Helvie, B. Sahiner, N. Petrick, D. D. Adler and M. M. Goodsitt, 'Classification of mass and normal breast tissue on digital mammograms: multiresolution texture analysis,' *Med. Phys.* **22**, 1501–1513 (1995).

[70] M. A. Goldberg, M. Pivovarov, W. W. Mayo-Smith, M. P. Bhalla, J. G. Blickman, R. T. Bramson, G. W. Boland, H. J. Llewellyn and E. Halpern, 'Application of wavelet compression to digitized radiographs,' *AJR Am. J. Roentgenol.* **163**, 463–468 (1994).

[71] A. H. Delaney and Y. Bresler, 'Multiresolution tomographic reconstruction using wavelets,' *IEEE Trans. Image Process.* **6**, 799–813 (1995).

[72] L. P. Panych and F. A. Jolesz, 'A dynamically adaptive imaging algorithm for wavelet-encoded MRI,' *Magn. Reson. Med.* **32**, 738–748 (1994).

[73] J. B. Weaver, X. Yansun, D. M. Healy, and J. R. Driscoll, 'Wavelet-encoded MR imaging,' *Magn. Reson. Med.* **24**, 275–287 (1992).

[74] J. B. Weaver, X. Yansun, D. M. Healy Jr. and L. D. Cromwell, 'Filtering noise from images with wavelet transforms,' *Magn. Reson. Med.* **21**, 288–295 (1991).

[75] D. M. Healy and J. B. Weaver, 'Two applications of wavelet transforms in magnetic resonance,' *IEEE Trans. Inform. Theory* **38**, 840–860 (1992).

[76] U. E. Ruttimann, M. Unser, D. Rio and R. R. Rawlings, 'Use of the wavelet transform to investigate differences in brain PET images between patients,' in *Proc. SPIE Conf. Mathemat. Methods in Med. Imag. II, Vol. 2035* (San Diego, July 1993), pp. 192–203.

[77] J. G. Daugman, 'Entropy reduction and decorrelation in visual coding by oriented neural receptive fields,' *IEEE Trans. Acoust., Biomed. Eng.* **36**, 107–114 (1989).

[78] L. Gaudart, J. Crebassa and J. P. Petrakian, 'Wavelet transform in human visual channels,' *Applied Optics* **32**, 4119–4127 (1993).

[79] M. Porst and Y. Y. Zeevi, 'Localized texture processing in vision: analysis and synthesis in Batorian space,' *IEEE Trans. Biomed. Eng.* **36**, 115–129 (1989).

[80] C. Tallon, O. Bertrand, P. Bouchet and J. Pernier, 'Gamma-range activity evoked by coherent visual stimuli in humans,' *Eur. J. Neurosci.* **7**, 1285–1291 (1995).

[81] A. Arneodo, Y. d'Aubenton-Carafa, E. Bacry, P. V. Graves, J. F. Muzy and C. Thermes, 'Wavelet based fractal analysis of DNA sequences,' *Physica D*

96, 291–320 (1996).

[82] A. A. Tsonis, P. Kumar, J. B. Elsner and P. A. Tsonis, 'Wavelet analysis of DNA sequences,' *Phys. Rev. E* **53**, 1828–1834 (1996).

[83] M. Unser and A. Aldroubi, 'A review of wavelets in biomedical applications,' in *Proceedings of the IEEE, Vol. 84, No. 4* (1996).

[84] A. Aldroubi and M. Unser, eds., *Wavelets in Medicine and Biology* (CRC Press, Boca Raton, 1996).

[85] M. Akay, 'Introduction: wavelet transforms in biomedical engineering,' *Ann. Biomed. Eng.* **23**, 529–530 (1995).

[86] M. Akay, 'Wavelets in biomedical engineering,' *Ann. Biomed. Eng.* **23**, 531–542 (1995).

[87] R. L. Stratonovich, *Topics in the theory of random noise, vol. I* (Gordon and Breach, New York, 1981).

[88] R. I. Kitney, D. Linkens, A. C. Selman and A. H. McDonald, *Automedica* **4**, 141–153 (1982).

[89] M. N. Levy, 'Sympathetic-parasympathetic interactions in the heart,' *Circ. Res.* **29**, 437–445 (1971).

[90] M. Malik and A. J. Camm, eds., *Heart rate variability* (Futura, Armonk NY, 1995).

[91] G. Sugihara, W. Allan, D. Sobel and K. D. Allan, 'Nonlinear control of heart rate variability in human infants,' *Proc. Natl. Acad. Sci. USA* **93**, 2608–2613 (1996).

[92] J. T. Bigger, Jr., C. A. Hoover, R. C. Steinman, L. M. Rolnitzky and J. L. Fleiss, 'Autonomic nervous system activity during myocardial ischemia in man estimated by power spectral analysis of heart period variability,' *Am. J. Cardiol.* **21**, 729–736 (1993).

[93] D. C. Michaels, E. P. Matyas and J. Jalife, 'A mathematical model of the effects of acetylcholine pulses on sino-atrial pacemaker activity,' *Circ. Res.* **55**, 89–101 (1984).

[94] C.-K. Peng, S. V. Buldyrev, J. H. Hausforff, S. Havlin, J. E. Mietus, M. Simons, H. E. Stanley, and A. L. Goldberger, 'Nonequilibrium dynamics as an indispensable characteristic of a healthy biological system,' *Integr. Physiol. Behavioral Sci.* **29**, 283–298 (1994).

[95] E. W. Montroll and M. F. Shlesinger, 'The wonderful world of random walks,' in *Nonequilibrium phenomena II: from stochastics to hydrodynamics*, edited by L. J. Lebowitz and E. W. Montroll (North-Holland, Amsterdam, 1984), pp. 1–121.

[96] D. Panter, *Modulation, noise and spectral analysis* (McGraw-Hill, New York, 1965).

[97] S. Akselrod, D. Gordon, F. A. Ubel, D. C. Shannon, A. C. Barger, and R. J. Cohen, 'Power spectrum analysis of heart rate fluctuation: a quantitative probe of beat-to-beat cardiovascular control,' *Science* **213**, 220–222 (1981).

[98] J. B. Bassingthwaighte, L. S. Liebovitch and B. J. West, *Fractal Physiology* (Oxford University Press, New York, 1994).

[99] A. Bezerianos, T. Bountis, G. Papaioannou, and P. Polydoropoulos, 'Nonlinear time series analysis of electrocardiograms,' *Chaos* **5**, 95–101 (1995).

[100] D. Hoyer, K. Schmidt, R. Bauer, U. Zwiener, M. Köhler, B. Lüthke, and M. Eiselt, 'Nonlinear analysis of heart rate and respiratory dynamics,' *IEEE Eng. Med. Bio.* **xx**, 31–39 (January/February 1997).

[101] A. Grossmann and J. Morlet, *Mathematics and physics: lectures on recent results* (World Scientific, Singapore, 1985).
[102] J. F. Muzy, E. Bacry and A. Arneodo, 'The multifractal formalism revisited with wavelets,' *Int. J. Bifurc. Chaos* **4**, 245–302 (1994).
[103] A. Arneodo, E. Bacry, P. V. Graves and J. F. Muzy, 'Characterizing long-range correlations in DNA sequences from wavelet analysis,' *Phys. Rev. Lett.* **74**, 3293–3296 (1995).
[104] L. A. Vainshtein and D. E. Vakman, *Separation of frequencies in the theory of oscillations and waves* (Nauka, Moscow, 1983).
[105] D. Gabor, 'Theory of communication,' *J. Inst. Elect. Engrs.* **93**, 429–457 (1946).
[106] *MIT-BIH polysomnographic database CD-ROM, second edition* (MIT-BIH Database Distribution, Cambridge, 1992), see Appendix B.
[107] C. Guilleminault, S. Connolly, R. Winkle, K. Melvin and A. Tilkian, 'Cyclical variation of the heart rate in sleep apnea syndrome,' *Lancet* **1**, 126–131 (1984).
[108] P. J. Strollo, Jr. and R. M. Rogers, 'Obstructive sleep apnea,' *N. Engl. J. Med.* **334**, 99–104 (1996).
[109] D. Stauffer and H. E. Stanley, *From Newton to Mandelbrot: a primer in theoretical physics, second edition* (Springer-Verlag, Heidelberg & New York, 1996).
[110] H. E. Stanley, *Introduction to phase transitions and critical phenomena* (Oxford University Press, London, 1971).
[111] T. Vicsek, *Fractal growth phenomena, second edition* (World Scientific, Singapore, 1992).
[112] A. A. Aghili, X. X. Rizwan-uddin, M. P. Griggin and J. R. Moorman, 'Scaling and ordering of neonatal rate variability,' *Phys. Rev. Lett.* **74**, 1254–1257 (1995).
[113] A. Bunde and S. Havlin, *Fractals in science* (Springer-Verlag, Berlin, 1994).
[114] G. L. Gerstein and B. B. Mandelbrot, 'Random walk models for the spike activity of a single neuron,' *Biophys. J.* **4**, 41–68 (1964)
[115] W. H. Press, *Numerical recipes in C: the art of scientific computing* (Cambridge University Press, Cambridge, 1988).
[116] L. A. Lipsitz, F. Hashimoto, L. Pl Lubowsky, J. E. Mietus, G. B. Moody, A. Appenzeller, and A. L. Goldberger, 'Heart rate and respiratory rhythm dynamics on ascent to high altitude,' *Br. Heart J.* **74**, 340–396 (1995).
[117] J. Theiler, S. Eubank, A. Longtin, B. Galdrikian and J. D. Farmer, 'Testing for nonlinearity in time series: the method of surrogate data,' *Physica D* **58**, 77–94 (1992).
[118] C.-K. Peng, S. V. Buldyrev, S. Havlin, M. Simons, H. E. Stanley and A. L. Goldberger, 'On the mosaic organization of DNA sequences,' *Phys. Rev. E* **49**, 1691–1695 (1994).
[119] P. Bak, C. Tang and K. Wiesenfeld, 'Self-organized criticality: an explanation of 1/f noise,' *Phys. Rev. Lett.* **59**, 381–384 (1987).
[120] L. P. Kadanoff, *From order to chaos* (World Scientific, Singapore, 1993).
[121] S. M. Ossadnik, S. V. Buldyrev, A. L. Goldberger, S. Havlin, R. N. Mantegna, C.-K. Peng, M. Simons and H. E. Stanley, 'Correlation approach to identify coding regions in DNA sequences,' *Biophys. J.* **67**, 64–70 (1994).
[122] J. M. Hausdorff, C.-K. Peng, Z. Ladin, J. Y. Wei and A. L. Goldberger, 'Is

walking a random walk? Evidence for long-range correlations in the stride interval of human gait,' *J. Appl. Physiol.* **78**, 349–358 (1995).

[123] A. L. Goldberger, D. R. Rigney, J. Mietus, E. M. Antman and M. Greenwald, 'Nonlinear dynamics in sudden cardiac death syndrome: heart rate oscillations and bifurcations,' *Experientia* **44**, 983–987 (1988).